Robustness of the Simulated Tropospheric Response to Ozone Depletion

WILLIAM J. M. SEVIOUR AND DARRYN W. WAUGH

Department of Earth and Planetary Sciences, The Johns Hopkins University, Baltimore, Maryland

LORENZO M. POLVANI

Lamont-Doherty Earth Observatory, Palisades, and Department of Applied Physics and Applied Mathematics, Columbia University, New York, New York

GUSTAVO J. P. CORREA

Lamont-Doherty Earth Observatory, Columbia University, Palisades, New York

CHAIM I. GARFINKEL

Fredy and Nadine Herrmann Institute of Earth Sciences, Hebrew University of Jerusalem, Jerusalem, Israel

(Manuscript received 16 November 2016, in final form 31 January 2017)

ABSTRACT

Recent studies have shown large intermodel differences in the magnitude of the simulated response of the Southern Hemisphere tropospheric circulation to ozone depletion. This inconsistency may be a result of different model dynamics, different ozone forcing, or statistical uncertainty. Here the summertime tropospheric response to ozone depletion is analyzed in an array of climate model simulations with incrementally increasing complexity. This allows the sensitivity of the response to a range of factors to be carefully tested, including the choice of model, the prescribed sea surface temperatures and greenhouse gas concentrations, the inclusion of a coupled ocean, the temporal resolution of the prescribed ozone concentrations, and the inclusion of interactive chemistry. A consistent poleward shift of the extratropical jet is found in all simulations. All simulations also show a strengthening of the extratropical jet and a widening of the southern edge of the Hadley cell, but the magnitude of these responses is much less consistent. However, in all simulations statistical uncertainty due to interannual variability is found to be large relative to the size of the response, despite considering long (100 yr) annually repeating simulations. It is therefore proposed that interannual variability is a dominant cause of intermodel differences in past studies, which have generally analyzed shorter, transient simulations.

1. Introduction

Since the mid-1970s, significant trends in the Southern Hemisphere summertime atmospheric circulation have been observed. Most notably, the extratropical jet has shifted poleward by approximately 2° latitude and strengthened (Swart and Fyfe 2012; Hande et al. 2012), a trend that is outside the range of natural variability found in the majority of coupled climate models (Thomas et al. 2015). At the same time there has also been a poleward expansion of the edge of the Hadley cell (Hu and Fu 2007; Seidel and Randel 2007; Davis and Rosenlof 2012). Several modeling studies have examined the roles of possible drivers of these trends, many of which have found stratospheric ozone depletion to be primarily responsible (Son et al. 2010; Polvani et al. 2011; Waugh et al. 2015; Schneider et al. 2015). However, others have found a smaller response to ozone depletion and concluded that warming sea surface temperatures (SSTs) play a larger role in driving these trends (Staten et al. 2012; Quan et al. 2014; Adam et al. 2014).

Gerber and Son (2014, hereafter GS14) quantified trends in the summertime austral jet latitude and Hadley cell extent in simulations from phases 3 and 5 of the

Corresponding author e-mail: William Seviour, wseviou1@jhu.edu

DOI: 10.1175/JCLI-D-16-0817.1

TABLE 1. Model integrations analyzed in this study and their forcings.

Pair name	Model	GHG	SST	Ozone	Length
CAM-2000	CAM3	2000	HadISST (2000)	SPARC 1960	100 yr
	—	—	—	SPARC 2000	—
CAM-1960	CAM3	1960	HadISST (1960)	SPARC 1960	100 yr
	—	—	—	SPARC 2000	—
CAM-1870	CAM3	1870	HadISST(1870)	SPARC 1960	50 yr
	—	—	—	SPARC 2000	—
CAM-1870CM2	CAM3	1870	CM2.1 control	SPARC 1960	50 yr
	—	—	—	SPARC 2000	—
GFDL-A	ESM2Mc A	1860	ESM2Mc control	SPARC 1960	100 yr
	—	—	—	SPARC 2000	—
GFDL-O	ESM2Mc	1860	Coupled	SPARC 1960	100 yr
	—	—	—	SPARC 2000	—
GFDL-MONTHLY	ESM2Mc	1860	Coupled	SPARC 1960	100 yr
	—	—	—	SD-WACCM monthly	—
GFDL-DAILY	ESM2Mc	1860	Coupled	SPARC 1960	100 yr
	—	—	—	SD-WACCM daily	—
GEOSCCM	GEOSCCM	Fixed/1994–2013	HadISST/Reynolds	Fixed ODS	5×20 yr
	—	1994–2013	—	Changing ODS	—
CMAM	CMAM	1960	Coupled	Chem. 1960–1975	3×16 yr
	—	—	—	Chem. 1995–2010	—

Coupled Model Intercomparison Projects (CMIP3 and CMIP5) and the Chemistry-Climate Model Validation activity 2 (CCMVal2). They found that some models simulated almost no trend in the jet position over 1960–99, while others showed as much as a 5° poleward shift (these large differences remained even after accounting for differences in the stratospheric response). They also found the CCMVal2 models to exhibit, on average, a stronger poleward shift than the CMIP3 or CMIP5 models, indicating that there may be systematic differences between different types of climate models. Several studies have proposed that these differences in model response to external forcing may be related to biases in model climatologies (Kidston and Gerber 2010; Barnes and Hartmann 2010; Garfinkel et al. 2013). More recently, however, Simpson and Polvani (2016) have argued that this relationship between climatology and response only exists in winter and so may have little influence on the tropospheric response to ozone depletion, which is largest in summer.

Multimodel studies (such as GS14) are limited by the fact that many different factors vary at once between model simulations (such as the ozone forcing, prescribed SSTs, dynamical core, etc.), so that it is difficult to attribute differences between model responses to any single factor. Here we investigate the robustness of the simulated tropospheric response to ozone depletion by analyzing an array of simulations with incrementally increasing complexity, ranging from an atmospheric model through to a coupled atmosphere–ocean model and a coupled model with interactive chemistry. These simulations are chosen so as to carefully isolate the following factors that may each contribute to differences in model responses: prescribed sea surface temperatures, greenhouse gas concentrations, the inclusion of a coupled ocean, the temporal resolution of the prescribed ozone concentrations, and the inclusion of interactive chemistry.

2. Model simulations

We analyze 10 pairs of simulations, summarized in Table 1, each of which compares conditions before and after significant ozone depletion. The first two pairs of simulations (CAM-2000 and CAM-1960), which use the Community Atmospheric Model version 3 (CAM3; Collins et al. 2006), are extended versions of simulations previously analyzed by Polvani et al. (2011) (their simulations were 50 years long rather than 100). These are atmosphere-only simulations with a horizontal resolution of T42 (roughly equivalent to a $2.8° \times 2.8°$ grid), and 26 hybrid vertical levels. Both simulations use sea ice concentrations and SSTs from the Hadley Centre Sea Ice and Sea Surface Temperature (HadISST) dataset (Rayner et al. 2003). CAM-2000 uses a climatological annual cycle of SST and sea ice calculated from the years 1992–2008, while CAM-1960 uses a climatology from 1952 to 1968. Additionally, CAM-2000 and CAM-1960 use greenhouse gas (GHG) concentrations for the years 2000 and 1960, respectively, from the Special Report on Emissions Scenarios (SRES) A1B scenario (Nakicenovic et al. 2000). To further test the sensitivity of the response

to ozone depletion upon the background SST and GHG concentrations two further 50-yr simulations have been performed with the CAM3 model: CAM-1870 and CAM-1870CM2. These both include preindustrial (1870) GHG concentrations and SSTs; CAM-1870 takes its SSTs from the HadISST dataset at the year 1870, while CAM-1870CM2 uses SSTs from a preindustrial control simulation of the Geophysical Fluid Dynamics Laboratory (GFDL) CM2.1 coupled model (Delworth et al. 2006).

The above comparisons considered a single atmospheric model. We assess the sensitivity to the choice of model by comparing CAM-1870CM2 with similar simulations (GFDL-A) that use an atmosphere-only version of the GFDL Earth System Model with Modular Ocean Model (ESM2Mc) (Gnanadesikan et al. 2015). This is a coarse-resolution version of GFDL ESM2M (Dunne et al. 2012), and has a horizontal resolution of 3.875° × 3° with 24 vertical levels. The GFDL-A simulations use annually repeating SSTs and sea ice concentrations that are very similar to those used in the CAM-1870CM2 simulations and taken from a coupled version of GFDL ESM2Mc.

To test the sensitivity of the response to the inclusion of a coupled ocean, we compare the GFDL-A simulations with simulations (GFDL-O) that use a coupled version of the same atmospheric model. The GFDL-O simulations use an ocean model with a 3° × 1.5° resolution with 28 vertical levels. Both GFDL-A and GFDL-O use preindustrial GHG concentrations, with a carbon dioxide concentration of 286 ppm, and simulations are run for 100 years.

These first six pairs of simulations each use ozone concentrations for the year 1960, before significant ozone depletion, and for the year 2000, after the formation of the Antarctic ozone hole. They use a zonal-mean, monthly-mean stratospheric ozone dataset developed by the International Global Atmospheric Chemistry (IGAC) and Stratosphere–Troposphere Processes and their Role in Climate (SPARC) activities (Cionni et al. 2011). This dataset, which we here refer to as the SPARC ozone dataset, was used in about half the models included in CMIP5. To test the sensitivity of the response to this choice of ozone dataset, we also analyze simulations (GFDL-MONTHLY) that use monthly-mean ozone concentrations derived from a 1995–2001 climatology of a specified dynamics version of the Whole Atmosphere Community Climate Model (SD-WACCM), in which temperatures and winds are nudged to meteorological reanalysis values but chemistry is calculated interactively (Solomon et al. 2015). Neely et al. (2014) have proposed that monthly averaging, as used in the SPARC ozone dataset and the GFDL-MONTHLY simulation, leads to an underestimate of the effects of ozone depletion. To test this we analyze a simulation with daily mean ozone concentrations (GFDL-DAILY), taken from the same SD-WACCM dataset as the GFDL-MONTHLY simulation.

In addition to the time-slice simulations described above we analyze two pairs of ensembles of simulations with interactive chemistry, meaning that ozone concentrations are calculated based on prescribed mixing ratios of chlorofluorocarbons and other ozone-depleting substances (ODSs). The first pair uses the Goddard Earth Observing System Chemistry-Climate Model (GEOSCCM; Pawson et al. 2008; Oman and Douglass 2014), an atmosphere-only model with horizontal resolution 2° × 2.5°, and 72 vertical levels. To isolate the effect of ozone depletion, we compare two 5-member ensembles of 20-yr simulations, one ensemble with ODSs fixed at 1960 mixing ratios and the other with observed time-evolving ODSs from 1994 to 2013. All simulations also use time-evolving GHG concentrations and SST from 1994 to 2013, except for two of the fixed-ODS simulations that use GHG concentrations fixed at a 1960 level. Sea ice and SST are prescribed from the HadISST dataset from 1994 to 2006, and from the Reynolds dataset (Reynolds et al. 2002) from 2007 to 2013. These simulations are described in greater detail by Aquila et al. (2016).

The final pair of simulations uses Canadian Middle Atmosphere Model (CMAM) simulations, which were previously described by McLandress et al. (2010). Like GEOSCCM, this is a chemistry–climate model, although now with the addition of a coupled ocean. These simulations use a T31 horizontal resolution (roughly equivalent to a 6° × 6° grid), with 71 vertical levels. To again isolate the role of ozone depletion, they use fixed 1960 GHG concentrations, aerosol, and solar forcing, but time-varying ODSs. We compare averages over two time periods, 1960–75 and 1995–2010, to reflect changes before and after significant ozone depletion.

3. Results

The effect of ozone depletion on zonal-mean temperature and wind is illustrated in Fig. 1 for the CAM-2000 pair of simulations. A strong cooling is seen in the austral polar lower stratosphere (Fig. 1a) and is largest during the spring, at the time of maximum ozone depletion. For the remainder of this study, we use the polar cap (60°–90°S) 100-hPa temperature averaged from October to January (ONDJ) T_{polar} as an index of the impact of ozone depletion on the stratosphere. This stratospheric cooling causes an intensification of the westerly winds in the polar stratosphere (Fig. 1b) and a poleward shift and intensification of the tropospheric

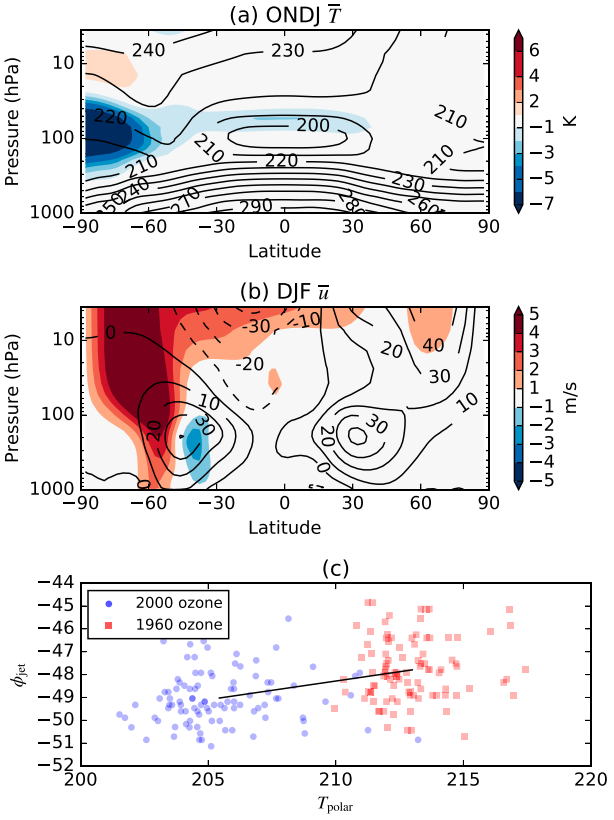

FIG. 1. (a) ONDJ zonal-mean temperature and (b) DJF zonal-mean zonal wind differences (colors) for the CAM-2000 simulations. The line contours represent the climatology for the 1960 ozone simulation. (c) The covariability of the DJF tropospheric jet latitude ϕ_{jet} and ONDJ polar cap (60°–90°S) temperature at 100 hPa, T_{polar}. The black line connects the means of the two distributions.

extratropical jet. Consistent with Thompson and Solomon (2002), we find the largest trends in the tropospheric jet to occur in summer, and so use the mean tropospheric jet position averaged from December to February (DJF). To account for differences in model resolution, the jet latitude ϕ_{jet} is determined as the location of the maximum of a quadratic fitted to the 850-hPa zonal-mean zonal wind at its maximum grid point and the two points either side. Visual inspection shows that a quadratic polynomial provides a good fit to the zonal-mean zonal wind for all simulations.

Figure 1c shows the relationship between ϕ_{jet} and T_{polar} for the CAM-2000 simulations, with each point representing a single year for each simulation. A clear cooling of the polar stratosphere and poleward shift of the tropospheric jet is seen under ozone depletion. However, there is also large interannual variability in both simulations, and the interannual correlation between ϕ_{jet} and T_{polar} is small ($r = 0.1$ for both simulations). In addition to jet latitude ϕ_{jet}, we also investigate the effect of ozone depletion upon the strength of the tropospheric jet $\overline{u}_{jet}$, and the edge of the Southern Hemisphere branch of the Hadley cell ϕ_{HC}. Note that $\overline{u}_{jet}$ is defined as the value of the quadratic fit to the zonal-mean zonal wind at ϕ_{jet}, and ϕ_{HC} is defined as the position where the DJF meridional mass streamfunction at 500 hPa first crosses zero south of the tropical maximum. To again account for differences in model resolution, this zero-crossing latitude is determined through linear interpolation.

Following the methodology described above for CAM-2000, the relationships between T_{polar} and ϕ_{jet}, $\overline{u}_{jet}$, and ϕ_{HC} for each pair of simulations are shown in Fig. 2. There are a wide range of climatological, pre-ozone depletion values of these parameters; ϕ_{jet} varies by about 12° latitude among models, ϕ_{HC} by about 10° latitude, $\overline{u}_{jet}$ by almost 3 m s^{-1}, and T_{polar} by about 8 K. These differences between model climatologies are significantly larger than the interannual variability of individual models. Note that the observed SH jet latitude is near 52°S (Swart and Fyfe 2012), indicating that the majority of models (except GEOSCCM) have an equatorward bias, as was also found in the majority of CMIP5 models (Wilcox et al. 2012; Bracegirdle et al. 2013). However, in contrast to Bracegirdle et al. (2013), we do not find a reduced equatorward bias in atmosphere-only relative to coupled versions of the same model; both GFDL-A and GFDL-O simulations have very similar jet latitudes. The effect of ozone depletion is broadly consistent across the models; the polar stratosphere is seen to cool and the extratropical jet shifts poleward and strengthens. The Hadley cell also expands poleward, although by less than the extratropical jet.

Figure 3 summarizes these changes resulting from ozone depletion in each of the simulation pairs. The horizontal bars represent the 95% uncertainty range for each difference, which is calculated by a bootstrap method in which individual years from each simulation are randomly resampled with replacement 10^4 times. Differences are then taken between these resampled simulations to produce a distribution of differences, and the uncertainty range is then that from the 2.5th to 97.5th percentiles of this distribution. These uncertainty ranges are a significant fraction of the response size for each variable. For example, even though the GFDL-O pair includes two 100-yr-long time-slice simulations, the uncertainty is approximately 17% of the response for ΔT_{polar}, 53% for $\Delta\phi_{jet}$, 67% for $\Delta\overline{u}_{jet}$, and about twice the response for $\Delta\phi_{HC}$, highlighting the large interannual variability present in these models.

It may be surprising that the stratospheric temperature response ΔT_{polar} for the GFDL-MONTHLY and GFDL-DAILY simulations is significantly smaller than

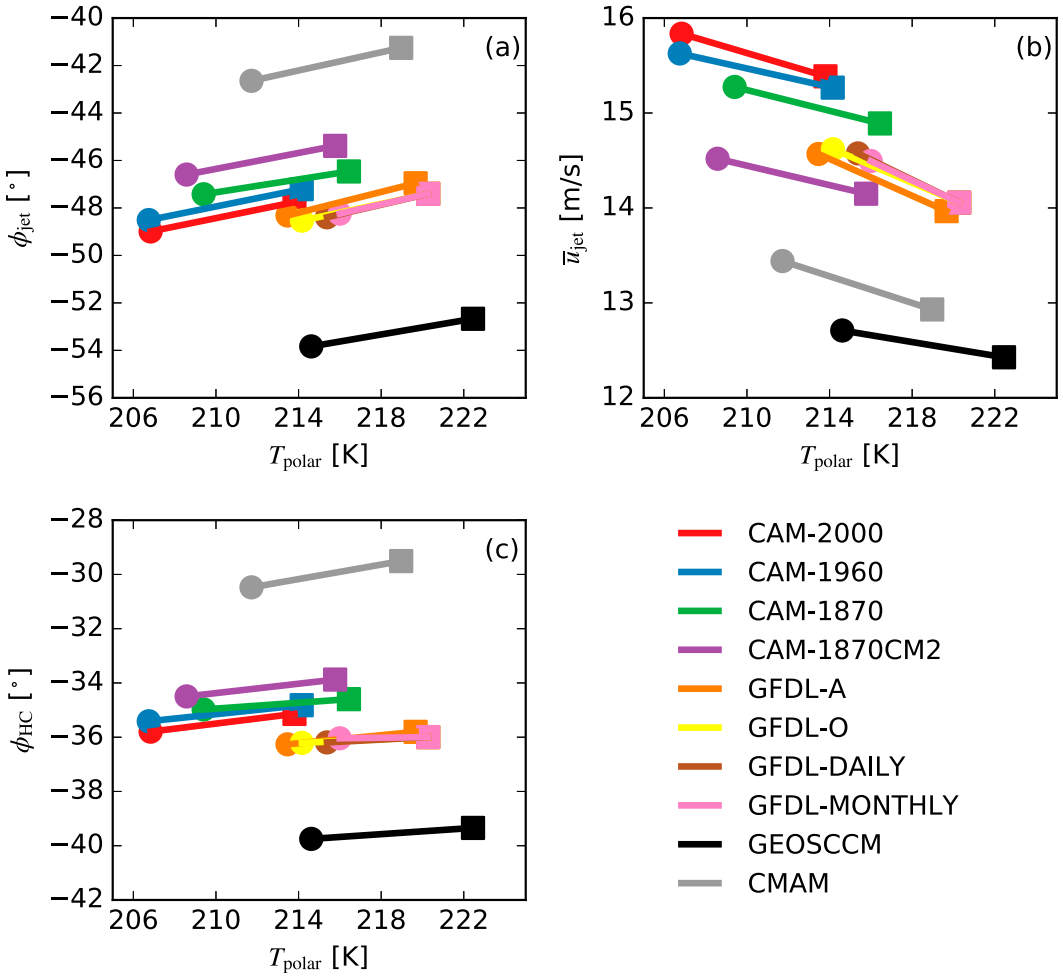

FIG. 2. Relation between ONDJ 100-hPa polar cap (60°–90°S) temperature T_{polar} and DJF average (a) tropospheric jet latitude ϕ_{jet}, (b) jet strength $\overline{u}_{jet}$, and (c) Hadley cell edge ϕ_{HC} for each of the model simulations. Squares represent simulations with year 1960 ozone and circles year 2000 ozone.

the GFDL-O and GFDL-A simulations (Fig. 3b), despite a relatively similar change in column ozone (Fig. 3a). We find that the SD-WACCM ozone dataset shows less ozone loss near 100 hPa than the SPARC dataset, thereby explaining the smaller temperature change at this level. However, their ozone loss is similar below 100 hPa and greater for SD-WACCM above 50 hPa, leading to similar column changes in the two datasets. Similarly, although CMAM has a lower column ozone change than other simulations, its ozone loss at 100 hPa is similar to the SPARC dataset. Hence, the temperature change at 100 hPa is also similar to simulations using the SPARC dataset.

The response of the jet latitude $\Delta\phi_{jet}$ is consistent across simulations, with a multimodel mean southward shift of 1.1° (Fig. 3c). The value of $\Delta\phi_{jet}$ for CAM-2000 (about 1.3°) is lower than that found by Polvani et al. (2011) (1.9°). On closer inspection we find the difference to be larger over the first 50 years of these simulations (1.7°), the period analyzed by Polvani et al. (2011), than the second 50 years (0.9°). This therefore explains most of the difference with Polvani et al. (2011) [the 1.7° value is still slightly less than the 1.9° found by Polvani et al. (2011), but this is likely due to methodological differences in the calculation of the jet latitude]. Neely et al. (2014) and Seviour et al. (2016) have shown tropospheric changes to be larger when ozone is specified with a daily temporal resolution, and indeed a slightly larger jet shift is seen in the GFDL-DAILY simulations relative to GFDL-MONTHLY. However, this difference is small relative to statistical uncertainty, again highlighting the large interannual variability present in these simulations.

To investigate whether these differences may be attributed to differences in the stratospheric response to ozone depletion, we normalize them by ΔT_{polar}, shown

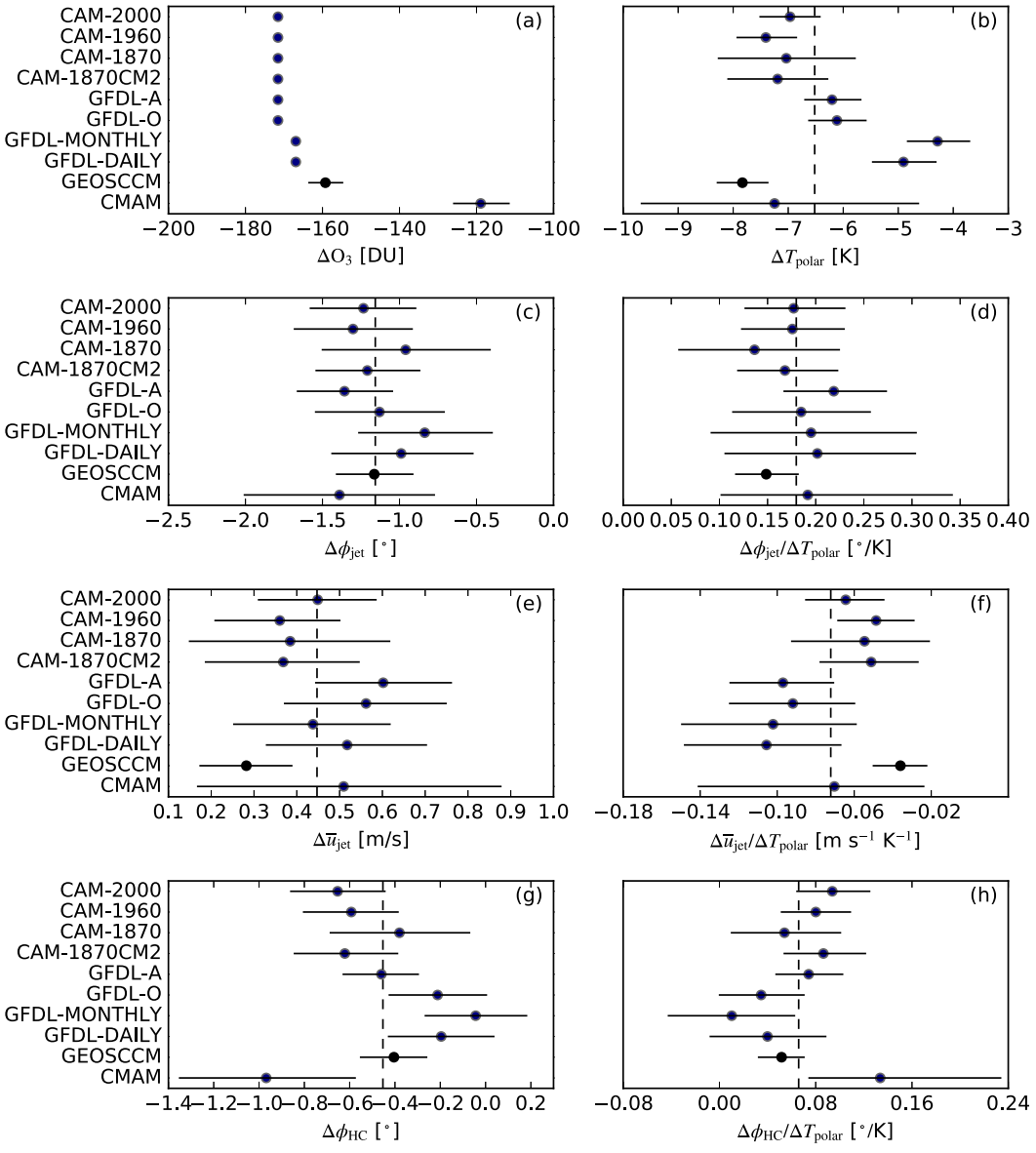

FIG. 3. Changes between simulations in (a) October mean polar cap (60°–90°S) column ozone ΔO_3, (b) ONDJ mean 100-hPa polar cap temperature ΔT_{polar}, (c) DJF tropospheric jet latitude $\Delta\phi_{jet}$, (e) jet strength $\Delta\overline{u}_{jet}$, and (g) Hadley cell edge $\Delta\phi_{HC}$. (d),(f),(h) As in (c),(e),(g), but for corresponding tropospheric responses normalized by ΔT_{polar}. Horizontal bars represent the 95% uncertainty range, determined by a bootstrap test, and dashed vertical lines show the multimodel mean.

in Figs. 3d, 3f, and 3h. This follows the analysis of GS14, who also assumed a linear relationship between ΔT_{polar} and $\Delta\phi_{jet}$ in the simulations they analyzed. Following this normalization, the spread among simulations in $\Delta\phi_{jet}$ is somewhat reduced. The multimodel mean value of $\Delta\phi_{jet}/\Delta T_{polar}$ is $0.18\,K^{-1}$, which falls within the intermodel spread of the regression coefficients found by GS14 for the historical and future CMIP3, CMIP5, and CCMVal2 simulations (approximately $0.05–0.5\,K^{-1}$).

In contrast to the results for $\Delta\phi_{jet}$, there is a much larger spread between models for $\Delta\overline{u}_{jet}$ and $\Delta\phi_{HC}$. Normalizing $\Delta\overline{u}_{jet}$ by ΔT_{polar} reveals a clear difference between the CAM3 simulations and GFDL ESM2Mc simulations, with the latter showing a greater strengthening of the vortex (Fig. 3f). This difference is consistent across simulations with different SST or GHG forcing as well as coupled and atmosphere-only simulations, indicating that it must arise from differences in the atmospheric dynamics of the two models. Despite these

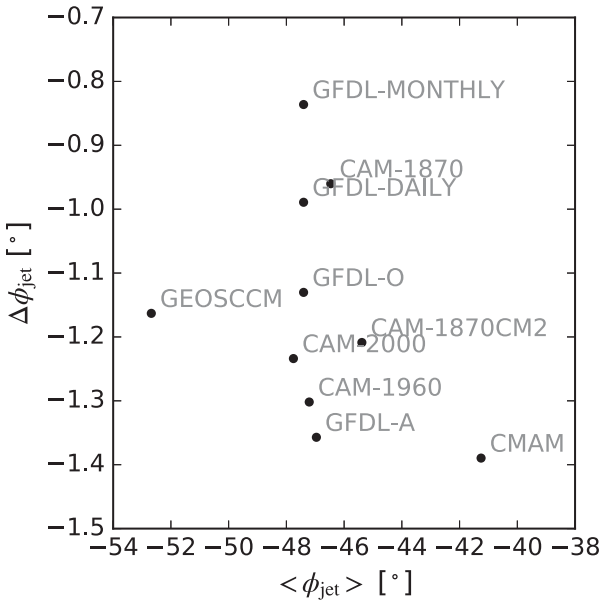

FIG. 4. Relationship between the mean DJF tropospheric jet latitude of the preozone depletion simulation $\langle\phi_{jet}\rangle$ and the jet shift under ozone depletion $\Delta\phi_{jet}$ for each of the simulations.

larger differences among simulations for Δu_{jet} and $\Delta\phi_{HC}$, the majority of simulations agree to within statistical uncertainty, particularly after normalizing by ΔT_{polar}, which again highlights the significant interannual variability present. The average value of $\Delta\phi_{HC}$ is a 0.45° poleward shift, approximately half that of $\Delta\phi_{jet}$, consistent with the 1:2 ratio reported by Kang and Polvani (2011).

Several studies have suggested that biases in the climatology of models may be linked to their sensitivity to external forcing (Kidston and Gerber 2010; Barnes and Hartmann 2010; Garfinkel et al. 2013). In Fig. 4 we test this relationship for our models, plotting the climatological average jet latitude $\langle\phi_{jet}\rangle$ against the jet shift $\Delta\phi_{jet}$ for each pair of simulations. It can be seen that there is little relationship between these two parameters, and indeed, there is not a statistically significant correlation ($r = -0.02$, $p = 0.4$, according to a two-tailed t test). This even applies for similar model types; for instance, the $\Delta\phi_{jet}$ for GFDL-A is almost twice that of GFDL-MONTHLY, but their two values of $\langle\phi_{jet}\rangle$ are within 0.5°. Furthermore, normalizing $\Delta\phi_{jet}$ by ΔT_{polar} does not lead to a significant correlation ($p = 0.2$). This result supports the findings of Simpson and Polvani (2016) that the jet position–jet shift relationship does not exist in summer.

4. Conclusions

In this study we have examined the summertime tropospheric response to stratospheric ozone depletion in a range of climate model simulations. We have analyzed 10 pairs of simulations, each representing conditions before and after significant ozone depletion. These models are of incrementally increasing complexity, ranging from an atmospheric model through to a coupled atmosphere–ocean model and a coupled model with interactive chemistry, and were chosen to test the sensitivity to a range of model parameters. We find that the poleward shift in the jet latitude is consistent among models, such that any differences are not statistically significant even among 100-yr-long simulations. The intensification of the jet and poleward expansion of the Hadley cell are less consistent, but interannual variability again leads to a large degree of uncertainty in the changes.

Given this apparent robust response, how can we explain the large differences in the jet response to ozone depletion found by GS14 in CMIP3, CMIP5, and CCMVal-2 models, even after normalizing by the stratospheric response (a range of approximately 0.05–0.5 K^{-1})? It is apparent from Fig. 3 that despite considering differences from long (50 or 100 yr) time slice simulations in this study, significant uncertainties in the jet responses remain, which are in some cases as large as the response itself. This can be attributed to the large interannual variability in the extratropical jet. Many of the historical and future simulations analyzed by GS14 consisted of just a single ensemble member, and would therefore be subject to even larger uncertainties. GS14 did not explicitly quantify uncertainties due to interannual variability in individual model responses, but they proposed that it is relatively unimportant compared to other sources of uncertainty (circulation sensitivity and forcing uncertainty). In contrast, the results presented here suggest that a significant fraction of intermodel differences found by GS14 could be attributed to interannual variability [although other factors such as the modeled location of the midlatitude oceanic front (Ogawa et al. 2015) are also likely to contribute to model diversity]. This highlights the importance of either large ensemble sizes or long time slice simulations in order to accurately quantify intermodel differences in the responses of the factors discussed in this study.

Acknowledgments. The authors thank three anonymous reviewers for their valuable comments. WJMS, DWW, LMP, and GJPC were funded by a Frontiers of Earth System Dynamics grant (FESD-1338814) from the U.S. National Science Foundation. CIG was supported by a European Research Council starting grant under the European Union's Horizon 2020 research and innovation programme (Grant Agreement 677756). Data from the simulations analyzed here are available from the authors on request.

REFERENCES

Adam, O., T. Schneider, and N. Harnik, 2014: Role of changes in mean temperatures versus temperature gradients in the recent widening of the Hadley circulation. *J. Climate*, **27**, 7450–7461, doi:10.1175/JCLI-D-14-00140.1.

Aquila, V., W. H. Swartz, D. W. Waugh, P. R. Colarco, S. Pawson, L. M. Polvani, and R. S. Stolarski, 2016: Isolating the roles of different forcing agents in global stratospheric temperature changes using model integrations with incrementally added single forcings. *J. Geophys. Res.*, **121**, 8067–8082, doi:10.1002/2015JD023841.

Barnes, E. A., and D. L. Hartmann, 2010: Testing a theory for the effect of latitude on the persistence of eddy-driven jets using CMIP3 simulations. *Geophys. Res. Lett.*, **37**, L15801, doi:10.1029/2010GL044144.

Bracegirdle, T. J., E. Shuckburgh, J. B. Sallee, Z. Wang, A. J. S. Meijers, N. Bruneau, T. Phillips, and L. J. Wilcox, 2013: Assessment of surface winds over the Atlantic, Indian, and Pacific Ocean sectors of the Southern Ocean in CMIP5 models: Historical bias, forcing response, and state dependence. *J. Geophys. Res.*, **118**, 547–562, doi:10.1002/jgrd.50153.

Cionni, I., and Coauthors, 2011: Ozone database in support of CMIP5 simulations: Results and corresponding radiative forcing. *Atmos. Chem. Phys.*, **11**, 11 267–11 292, doi:10.5194/acp-11-11267-2011.

Collins, W. D., and Coauthors, 2006: The Community Climate System Model version 3 (CCSM3). *J. Climate*, **19**, 2122–2143, doi:10.1175/JCLI3761.1.

Davis, S. M., and K. H. Rosenlof, 2012: A multidiagnostic intercomparison of tropical-width time series using reanalyses and satellite observations. *J. Climate*, **25**, 1061–1078, doi:10.1175/JCLI-D-11-00127.1.

Delworth, T. L., and Coauthors, 2006: GFDL's CM2 global coupled climate models. Part I: Formulation and simulation characteristics. *J. Climate*, **19**, 643–674, doi:10.1175/JCLI3629.1.

Dunne, J. P., and Coauthors, 2012: GFDL's ESM2 global coupled climate–carbon Earth system models. Part I: Physical formulation and baseline simulation characteristics. *J. Climate*, **25**, 6646–6665, doi:10.1175/JCLI-D-11-00560.1.

Garfinkel, C. I., D. W. Waugh, and E. P. Gerber, 2013: The effect of tropospheric jet latitude on coupling between the stratospheric polar vortex and the troposphere. *J. Climate*, **26**, 2077–2095, doi:10.1175/JCLI-D-12-00301.1.

Gerber, E. P., and S.-W. Son, 2014: Quantifying the summertime response of the austral jet stream and Hadley cell to stratospheric ozone and greenhouse gases. *J. Climate*, **27**, 5538–5559, doi:10.1175/JCLI-D-13-00539.1.

Gnanadesikan, A., M.-A. Pradal, and R. Abernathey, 2015: Isopycnal mixing by mesoscale eddies significantly impacts oceanic anthropogenic carbon uptake. *Geophys. Res. Lett.*, **42**, 4249–4255, doi:10.1002/2015GL064100.

Hande, L. B., S. T. Siems, and M. J. Manton, 2012: Observed trends in wind speed over the Southern Ocean. *Geophys. Res. Lett.*, **39**, L11802, doi:10.1029/2012GL051734.

Hu, Y., and Q. Fu, 2007: Observed poleward expansion of the Hadley circulation since 1979. *Atmos. Chem. Phys.*, **7**, 5229–5236, doi:10.5194/acpd-7-9367-2007.

Kang, S. M., and L. M. Polvani, 2011: The interannual relationship between the latitude of the eddy-driven jet and the edge of the Hadley cell. *J. Climate*, **24**, 563–568, doi:10.1175/2010JCLI4077.1.

Kidston, J., and E. P. Gerber, 2010: Intermodel variability of the poleward shift of the austral jet stream in the CMIP3 integrations linked to biases in 20th century climatology. *Geophys. Res. Lett.*, **37**, L09708, doi:10.1029/2010GL042873.

McLandress, C., A. I. Jonsson, D. A. Plummer, M. C. Reader, J. F. Scinocca, and T. G. Shepherd, 2010: Separating the dynamical effects of climate change and ozone depletion. Part I: Southern Hemisphere stratosphere. *J. Climate*, **23**, 5002–5020, doi:10.1175/2010JCLI3586.1.

Nakicenovic, N., and Coauthors, 2000: *Emissions Scenarios*. Cambridge University Press, 570 pp.

Neely, R. R., D. R. Marsh, K. L. Smith, S. M. Davis, and L. M. Polvani, 2014: Biases in Southern Hemisphere climate trends induced by coarsely specifying the temporal resolution of stratospheric ozone. *Geophys. Res. Lett.*, **41**, 8602–8610, doi:10.1002/2014GL061627.

Ogawa, F., N.-E. Omrani, K. Nishii, H. Nakamura, and N. Keenlyside, 2015: Ozone-induced climate change propped up by the Southern Hemisphere oceanic front. *Geophys. Res. Lett.*, **42**, 10 056–10 063, doi:10.1002/2015GL066538.

Oman, L. D., and A. R. Douglass, 2014: Improvements in total column ozone in GEOSCCM and comparisons with a new ozone-depleting substances scenario. *J. Geophys. Res. Atmos.*, **119**, 5613–5624, doi:10.1002/2014JD021590.

Pawson, S., R. S. Stolarski, A. R. Douglass, P. A. Newman, J. E. Nielsen, S. M. Frith, and M. L. Gupta, 2008: Goddard Earth Observing System chemistry–climate model simulations of stratospheric ozone–temperature coupling between 1950 and 2005. *J. Geophys. Res. Atmos.*, **113**, D12103, doi:10.1029/2007JD009511.

Polvani, L. M., D. W. Waugh, G. J. P. Correa, and S.-W. Son, 2011: Stratospheric ozone depletion: The main driver of twentieth-century atmospheric circulation changes in the Southern Hemisphere. *J. Climate*, **24**, 795–812, doi:10.1175/2010JCLI3772.1.

Quan, X.-W., M. P. Hoerling, J. Perlwitz, H. F. Diaz, and T. Xu, 2014: How fast are the tropics expanding? *J. Climate*, **27**, 1999–2013, doi:10.1175/JCLI-D-13-00287.1.

Rayner, N. A., D. E. Parker, E. B. Horton, C. K. Folland, L. V. Alexander, D. P. Rowell, E. C. Kent, and A. Kaplan, 2003: Global analyses of sea surface temperature, sea ice, and night marine air temperature since the late nineteenth century. *J. Geophys. Res.*, **108** (D14), 4407, doi:10.1029/2002JD002670.

Reynolds, R. W., N. A. Rayner, T. M. Smith, D. C. Stokes, and W. Wang, 2002: An improved in situ and satellite SST analysis for climate. *J. Climate*, **15**, 1609–1625, doi:10.1175/1520-0442(2002)015<1609:AIISAS>2.0.CO;2.

Schneider, D. P., C. Deser, and T. Fan, 2015: Comparing the impacts of tropical SST variability and polar stratospheric ozone loss on the Southern Ocean westerly winds. *J. Climate*, **28**, 9350–9372, doi:10.1175/JCLI-D-15-0090.1.

Seidel, D. J., and W. J. Randel, 2007: Recent widening of the tropical belt: Evidence from tropopause observations. *J. Geophys. Res.*, **112**, D20113, doi:10.1029/2007JD008861.

Seviour, W. J. M., A. Gnanadesikan, and D. W. Waugh, 2016: The transient response of the Southern Ocean to stratospheric ozone depletion. *J. Climate*, **29**, 7383–7396, doi:10.1175/JCLI-D-16-0198.1.

Simpson, I. R., and L. M. Polvani, 2016: Revisiting the relationship between jet position, forced response, and annular mode variability in the southern mid-latitudes. *Geophys. Res. Lett.*, **43**, 2896–2903, doi:10.1002/2016GL067989.

Solomon, S., D. Kinnison, J. Bandoro, and R. Garcia, 2015: Simulation of polar ozone depletion: An update. *J. Geophys. Res. Atmos.*, **120**, 7958–7974, doi:10.1002/2015JD023365.

Son, S.-W., and Coauthors, 2010: Impact of stratospheric ozone on Southern Hemisphere circulation change: A multimodel assessment. *J. Geophys. Res.*, **115**, D00M07, doi:10.1029/2010JD014271.

Staten, P. W., J. J. Rutz, T. Reichler, and J. Lu, 2012: Breaking down the tropospheric circulation response by forcing. *Climate Dyn.*, **39**, 2361–2375, doi:10.1007/s00382-011-1267-y.

Swart, N. C., and J. C. Fyfe, 2012: Observed and simulated changes in the Southern Hemisphere surface westerly wind-stress. *Geophys. Res. Lett.*, **39**, L16711, doi:10.1029/2012GL052810.

Thomas, J. L., D. Waugh, and A. Gnanadesikan, 2015: Decadal variability in the Southern Hemisphere extratropical circulation: Recent trends and natural variability. *Geophys. Res. Lett.*, **42**, 5508–5515, doi:10.1002/2015GL064521.

Thompson, D. W. J., and S. Solomon, 2002: Interpretation of recent Southern Hemisphere climate change. *Science*, **296**, 895–899, doi:10.1126/science.1069270.

Waugh, D. W., C. I. Garfinkel, and L. M. Polvani, 2015: Drivers of the recent tropical expansion in the Southern Hemisphere: Changing SSTs or ozone depletion? *J. Climate*, **28**, 6581–6586, doi:10.1175/JCLI-D-15-0138.1.

Wilcox, L. J., A. J. Charlton-Perez, and L. J. Gray, 2012: Trends in austral jet position in ensembles of high- and low-top CMIP5 models. *J. Geophys. Res.*, **117**, D13115, doi:10.1029/2012JD017597.